



# Synthesis, structure and properties of a fumarate bridged Ni(II) coordination polymer

Sanchay J. Bora<sup>1</sup>, Birinchi K. Das<sup>\*</sup>

Department of Chemistry, Gauhati University, Guwahati 781 014, India

## ARTICLE INFO

### Article history:

Received 14 March 2011  
Received in revised form 20 May 2011  
Accepted 21 May 2011  
Available online 13 June 2011

### Keywords:

1-D coordination polymer  
Nickel(II) fumarate  
4-Cyanopyridine ligand  
Graph-set analysis  
Metallo-supramolecular assembly

## ABSTRACT

A 1-D coordination polymer *catena*[ $\mu$ -fumaratobis(4-cyanopyridine)diaquanickel(II)],  $[\text{Ni}(\mu\text{-C}_4\text{H}_2\text{O}_4)(4\text{-CNpy})_2(\text{H}_2\text{O})_2]_n$  **1** has been synthesized and structurally characterized. Compound **1** is monoclinic,  $P2_1/c$  with unit cell parameters  $a = 8.8759(9)$  Å,  $b = 11.4112(11)$  Å,  $c = 8.8908(9)$  Å,  $\beta = 106.010(6)^\circ$ ,  $V = 865.6(1)$  Å<sup>3</sup>,  $Z = 2$  and  $D_{\text{calc.}} = 1.600$  g cm<sup>-3</sup>. The structure refined to  $R_1 = 0.0245$ ,  $wR_2 = 0.0626$  for all 2014 unique reflections and 152 parameters;  $\text{GoF} = 1.056$ . It consists of a polymeric chain of nearly octahedral Ni<sup>2+</sup> centers bridged by bidentate fumarate ligands. Non-covalent interactions lead these chains to aggregate into an interesting metallo-supramolecular assembly. Indexed PXRD pattern, solid state UV–vis–NIR spectral data, thermogravimetric behavior and variable temperature magnetic susceptibility data on **1** are presented.

© 2011 Elsevier B.V. All rights reserved.

## 1. Introduction

Coordinated ligand systems containing electron donor and acceptor sites lead to metallo-supramolecular assemblies [1], and in this context 4-cyanopyridine (4-CNpy) with the electron-withdrawing nitrile group as the acceptor and the pyridyl nitrogen as the donor represents a suitable candidate [2]. Presence of two regions of delocalized electron density also brings in the possibility of  $\pi$ – $\pi$  interactions so as to direct preferences for thermodynamically favoured solid state structures [3,4]. On the other hand, presence of the dianion of fumaric acid ( $\text{C}_4\text{H}_2\text{O}_4^{2-}$ ) as a ligand in metal organic compounds is known to give coordination polymers of various dimensionalities [5,6]. Coordination polymer is a family which is composed of 1-D chains, 2-D sheets, and 3-D frameworks of building blocks connected via metal ligand coordination bonds. Hydrogen bonding and  $\pi$ – $\pi$  stacking interaction may further be utilized to generate low-dimensional coordination polymers into supramolecular networks of higher dimensionality.

Coordination polymers based on transition metals and multi-functional organic ligands have received considerable recent attention in the design of supramolecular assemblies having potential applications in diverse fields such as catalysis, cooperative magnetism, luminescence, NLO behavior, electrical conductivity, among others [7]. It is also a notable fact that such compounds have been

described as promising materials for gas sorption as well as storage [8,9]. These compounds have also been described as precursors for the synthesis of nanomaterials [10,11]. In this paper we describe our results on the synthesis, crystal structure determination and properties of a new 1-D coordination polymer of Ni(II), formulated as  $[\text{Ni}(\mu\text{-C}_4\text{H}_2\text{O}_4)(4\text{-CNpy})_2(\text{H}_2\text{O})_2]_n$  **1**.

## 2. Experimental

### 2.1. Materials

Reagents and solvents used in this work were used as obtained from commercial sources. Disodium fumarate was prepared by evaporating a NaOH-neutralized aqueous solution of fumaric acid. The off-white residue so obtained was dried at 110 °C.  $\text{Ni}(\text{H}_2\text{O})_3(\text{SO}_4)(4\text{-CNpy})_2 \cdot \text{H}_2\text{O}$  has been prepared by following a published method [12].

### 2.2. Instrumentation

The C,H,N analysis was performed using a Perkin–Elmer 2400 Series II CHNS/O Analyzer. FT-IR spectra were recorded in a Perkin–Elmer RX1 spectrophotometer in the mid-IR region (4000–400 cm<sup>-1</sup>) for KBr pellets. The solid state UV–vis–NIR (240–2600 nm) spectra were obtained using a Hitachi U-4100 spectrophotometer equipped with an integrating sphere. BaSO<sub>4</sub> powder was used as reference (100% reflectance). Absorption data were calculated from the diffuse reflectance data using the Kubelka–Munk function ( $a/S = (1 - R)^2/2R$  where  $a$  is the absorption

<sup>\*</sup> Corresponding author. Tel.: +91 361 2570535; fax: +91 361 2700311.

E-mail addresses: [snachay.bora@gmail.com](mailto:snachay.bora@gmail.com) (S.J. Bora), [das\\_bk@rediffmail.com](mailto:das_bk@rediffmail.com) (B.K. Das).

<sup>1</sup> Present address: Pandu College, Guwahati 781 012, India.

**Table 1**  
Crystal data and structure refinement for  $[\text{Ni}(\mu\text{-C}_4\text{H}_2\text{O}_4)(4\text{-CNpy})_2(\text{H}_2\text{O})_2]_n$  **1**.

Empirical formula, <i>FW</i>	$\text{C}_{16}\text{H}_{14}\text{N}_4\text{O}_6\text{Ni}$ , 417.02
Crystal system, space group	Monoclinic, $P2_1/c$
Unit cell dimensions	$a = 8.8759(9)$ Å $b = 11.4112(11)$ Å $c = 8.8908(9)$ Å $\beta = 106.010(6)^\circ$
Volume	$865.57(15)$ Å <sup>3</sup>
<i>Z</i> , Calculated density	2, 1.600 g/cm <sup>3</sup>
Absorption coefficient	$1.164$ mm <sup>-1</sup>
Crystal size	$0.38 \times 0.27 \times 0.17$ mm <sup>3</sup>
Ratio of $T_{\min}$ , $T_{\max}$	0.86113
$\theta$ range for data collection	$2.39\text{--}28.34^\circ$
<i>hkl</i> ranges	<i>h</i> : $-11 \rightarrow 11$ ; <i>k</i> : $-15 \rightarrow 12$ ; <i>l</i> : $-11 \rightarrow 11$
Reflections collected/unique	6594/2014 [ <i>R</i> (int) = 0.0193]
Data/restraints/parameters	2014/0/152
<i>R</i> indices <sup>a</sup> [all data]	$R_1 = 0.0245$ , $wR_2 = 0.0626$
Goodness-of-fit <sup>b</sup> on $F^2$	1.056
(Shift/s.u.) <sub>max</sub>	0.000
Largest diff. peak and hole	0.286 and $-0.325$ e Å <sup>-3</sup>

<sup>a</sup>  $wR_2 = \{ \sum [ w(F_o^2 - F_c^2)^2 ] / \sum [ w(F_o^2)^2 ] \}^{1/2}$ ;  $R_1 = \sum ||F_o| - |F_c|| / \sum |F_o|$ .

<sup>b</sup>  $\text{Goof} = S = \{ \sum [ w(F_o^2 - F_c^2)^2 ] / (n - p) \}^{1/2}$ .

coefficient, *R* the reflectance and *S* the scattering coefficient). Thermogravimetric studies were carried out under a flow of N<sub>2</sub> gas using a Mettler Toledo TGA/DSC1 STAR<sup>e</sup> system at a heating rate of 10 °C min<sup>-1</sup>. Room temperature magnetic susceptibilities were measured at 300 K on a Sherwood Mark 1 Magnetic Susceptibility Balance by Evans Method. Variable temperature magnetic susceptibility data on compound **1** were measured using an MPMS Quantum Design SQUID magnetometer at a constant magnetic field of 1000G. The initial 'moment' data given by the computer controlled instrument were analyzed according to standard formulae of magnetochemistry using *Origin 8.0* [13].

### 2.3. Synthesis of $[\text{Ni}(\mu\text{-C}_4\text{H}_2\text{O}_4)(4\text{-CNpy})_2(\text{H}_2\text{O})_2]_n$ **1**

About 0.9 g (2 mmol) of  $\text{Ni}(\text{H}_2\text{O})_3(\text{SO}_4)(4\text{-CNpy})_2 \cdot \text{H}_2\text{O}$  [11] was dissolved in 20 mL of water to obtain a light green solution. To that resulting solution 0.32 g (2 mmol) of disodium fumarate was added and the mixture was stirred mechanically for 2 h. The sky blue precipitate formed was filtered, washed with small volumes of water under suction and then with methanol and dried in a vacuum desiccator over fused CaCl<sub>2</sub>. Yield: 0.58 g (70%). Anal. calcd. for  $\text{C}_{16}\text{H}_{14}\text{N}_4\text{O}_6\text{Ni}$ : C, 46.04%; H, 3.36%; N, 13.43%. Found: C,

**Table 2**  
Selected geometric parameters for compound **1**.

Bond distances (Å) and angles (°)			
M(1)—O(2)	2.031(1)	O(2) <sup>a</sup> —M(1)—O(1)	89.95(4)
M(1)—O(1)	2.098(1)	O(2)—M(1)—O(1)	90.05(4)
M(1)—N(1)	2.119(1)	O(2)—M(1)—N(1)	92.00(4)
O(2)—C(7)	1.260(2)	O(1) <sup>a</sup> —M(1)—N(1)	92.57(4)
O(3)—C(7)	1.256(2)	O(1)—M(1)—N(1)	87.43(4)
N(1)—C(1)	1.342(2)	O(2)—M(1)—N(1) <sup>a</sup>	88.00(4)
Hydrogen bonds			
D—H...A	d(H...A)	d(D...A)	∠(DHA)
O(1)—H(7)...O(3)	1.96(2)	2.685(1)	157(2)
O(1)—H(6)...O(3) <sup>b</sup>	1.95(2)	2.773(1)	177(2)

Symmetry codes:  $a = -x + 1, -y, -z$ ;  $b = x, -y - 1/2, z - 1/2$ .

46.84%; H, 3.46%; N, 13.87%. IR spectral data (KBr disc, cm<sup>-1</sup>): 3108(s), 2242(s), 1968(m), 1870(w), 1718(sh), 1608(sh), 1542(s), 1416(sh), 1384(s), 1220(s), 1126(w), 1098(m), 1070(s), 1020(m), 988(s), 864(sh), 838(m), 808(m), 770(m), 684(s), 596(m), 566(s) [s, strong; m, medium; w, weak; br, broad; sh, shoulder].  $\mu_{\text{eff}} = 3.08$  BM.

### 2.4. X-ray crystallography

Molecular and crystal structure of **1** was determined by single crystal X-ray diffraction technique. Suitable crystals of **1** were obtained upon slow evaporation of the preparative reaction mixtures obtained as above. The chosen crystals of suitable size were mounted on a glass fiber for intensity data collection at room temperature using graphite monochromatized Mo K $\alpha$  radiation (0.7107 Å) on a Bruker SMART CCD Diffractometer [14]. Crystal structures were solved by direct methods (*SHELXS*) and refined by full-matrix least squares techniques (*SHELXL*) with *SHELX-97* [15] using the *WinGX* [16] platform available for personal computers. The hydrogen atoms in compound **1** were located in difference Fourier maps and refined with isotropic atomic displacement parameters. Crystallographic data for **1** are presented in Table 1. The structural diagrams were drawn using *ORTEP-3 for Windows* [17] and *Diamond* [18].

Powder X-ray diffraction patterns in the 3–60° 2 $\theta$ -range were recorded on a Philips X'Pert PRO instrument using Cu K $\alpha$  radiation (1.5418 Å) at a scan rate of 0.5 s (0.5° 2 $\theta$ ) per step at 40 kV/30 mA. The calculated diffraction patterns assuming Bragg–Brentano geometry were obtained from results of single crystal structure analyses using the computer program *PowderCell* [19].

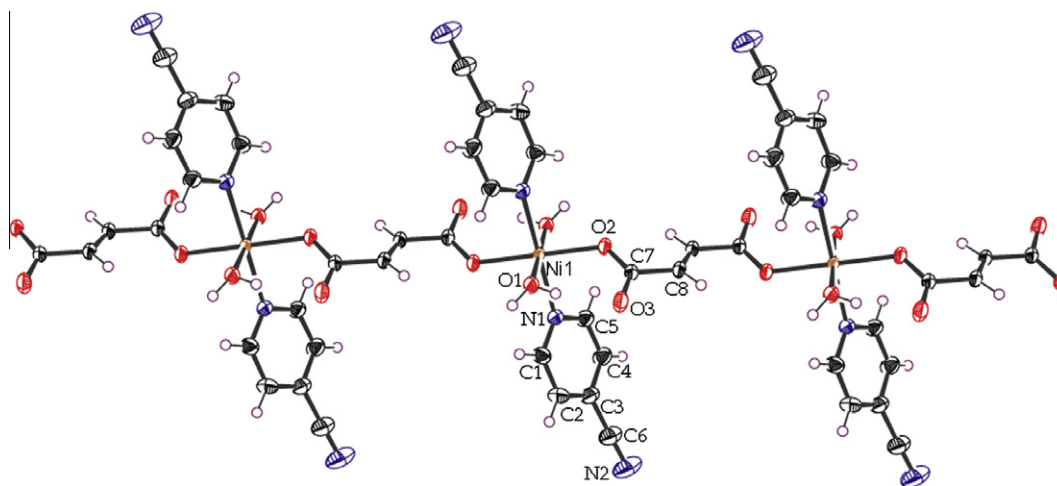


**Fig. 1.** ORTEP diagram of a section of the polymeric chain of **1** with non-hydrogen atoms drawn as 50% probability ellipsoids.

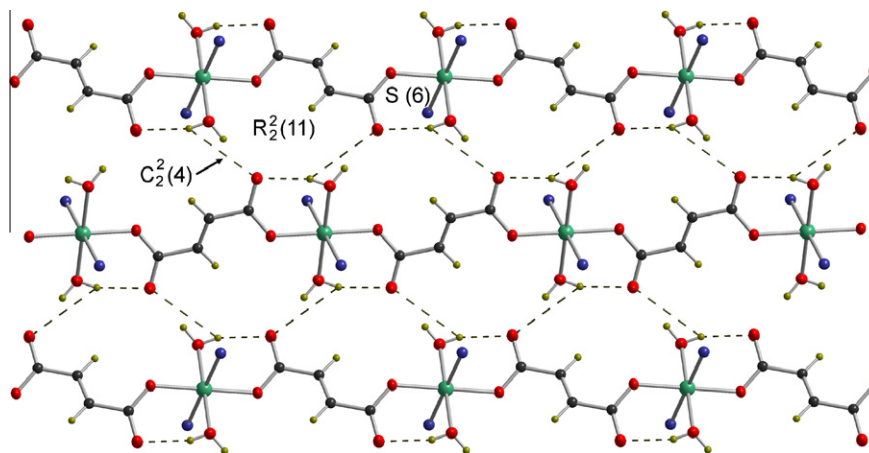


**Fig. 2.** Inter-chain and intra-chain hydrogen bonding interactions observed in the crystal structure of **1**. Graph-set notations are indicated. For clarity, the 4-CNpy ligands have been shown only by their pyridyl N atoms.

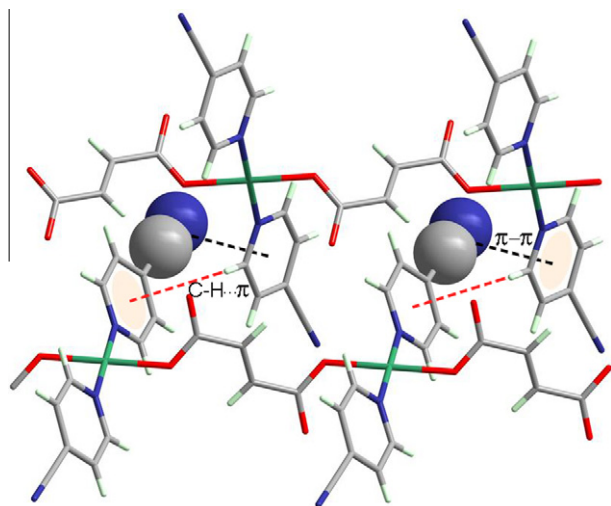


**Fig. 3.**  $\pi$ - $\pi$  interaction observed for  $-\text{C}\equiv\text{N}$  fragments with pyridyl rings and  $\text{C}-\text{H}\cdots\pi$  interaction between pyridyl ring hydrogen and aromatic  $\pi$ -systems.

### 3. Results and discussion

#### 3.1. Synthesis

Compound **1** of composition  $[\text{Ni}(\mu\text{-C}_4\text{H}_2\text{O}_4)(4\text{-CNpy})_2(\text{H}_2\text{O})_2]_n$  **1** can be prepared in good yield by adding one equivalent of the disodium salt of fumaric acid,  $\text{Na}(\text{C}_4\text{H}_2\text{O}_4)$ , to an aqueous solution of  $[\text{Ni}(\text{H}_2\text{O})_3(4\text{-CNpy})_2(\text{SO}_4)]\cdot\text{H}_2\text{O}$  [12] and stirring the mixture at room temperature. Sky blue crystals of **1** can be obtained on slow evaporation of the said reaction mixture. The non-hygroscopic solid is sparingly soluble in water as well as common organic solvents. Crystals of **1** remain indefinitely stable against dehydration under ambient conditions.

#### 3.2. Crystal structure

The title compound  $[\text{Ni}(\mu\text{-C}_4\text{H}_2\text{O}_4)(4\text{-CNpy})_2(\text{H}_2\text{O})_2]_n$  **1** is a linear one-dimensional coordination polymer wherein the fumarate dianion ( $\text{C}_4\text{H}_2\text{O}_4^{2-}$ ) bridges the nearly octahedral  $\text{Ni}^{2+}$  ions in a centrosymmetric fashion (Fig. 1). Table 2 presents the geometrical data on the crystal structure.

The chain polymers run along the  $c$ -axis in the crystal structure of **1**. The observed  $\text{Ni}(1)-\text{N}(1)$  distance of 2.119(1) Å for **1** is comparable to the corresponding distance of 2.165(1) Å in  $[\text{Ni}(\text{H}_2\text{O})_4(4\text{-CNpy})_2]\cdot(\text{BPh}_4)_2\cdot 2(4\text{-CNpy})\cdot 4\text{H}_2\text{O}$  [2]. The distances  $\text{Ni}(1)-\text{O}(3) = 3.316(1)$  Å for the uncoordinated O-atoms of the carboxyl groups confirm the presence of fumarate ions in monodenate coordination mode in the polymeric chains of the compound.  $\text{Ni}^{2+}$  ion is present in a distorted octahedral environment where the angles subtended at the metal center vary from  $87.65(4)^\circ$  to  $92.35(4)^\circ$ . A cobalt(II) compound  $[\text{Co}(\mu\text{-fumarato})(\gamma\text{-methylpyridine})_2(\text{H}_2\text{O})_2]_\infty$  reported by Zhang et al. [20] is structurally similar with **1**. However,  $\text{Mn}(\mu\text{-C}_4\text{H}_2\text{O}_4)(\text{phen})(\text{H}_2\text{O})_2$  was found to be a zig-zag 1-D polymer [21] due to the presence of the bidentate ligand. The  $\text{Ni}\cdots\text{Ni}$  distance of **1** is 8.891(1) Å which is significantly low compared to the corresponding values of 9.728 Å and 9.730 Å reported for the fumarate bridged dimers  $[\text{Ni}(\text{C}_4\text{H}_2\text{O}_4)(\text{bpp})(\text{H}_2\text{O})]'$  ( $\text{bpp} = 1,3\text{-bis}(4\text{-pyridyl})\text{propane}$ ) [6] and  $[\text{Ni}_2(\text{C}_4\text{H}_2\text{O}_4)(\text{phen})_4(\text{H}_2\text{O})_2]\cdot\text{C}_4\text{H}_2\text{O}_4\cdot 16\text{H}_2\text{O}$  [22] ( $\text{phen} = 1,10\text{-phenanthroline}$ ) respectively.

Extensive hydrogen bonding interactions between the uncoordinated O-atoms (fumarate) and the coordinated water molecules are observed in the crystal structure of **1**. The hydrogen bonding network is extended via intra-chain as well as inter-chain links which give rise to a 2-D supramolecular architecture (Fig. 2). The hydrogen bond parameters are given in Table 2. The hydrogen bonding interactions in **1** can be analyzed by making use of Graph Set Theory [23]. The coordinated water molecules and the uncoordinated carboxyl oxygen atoms are self-assembled to form supramolecular chains that run approximately along the direction of the polymers in the crystal lattice. In graph set notation such a chain is describable as  $\text{C}_2^2(4)$  where the subscripts and superscripts are the number of hydrogen bond donors and acceptors respectively. A 11-membered hydrogen-bonded  $\text{R}_2^2(11)$  ring identified as  $(\text{OH})_{\text{aqua}}-\text{O}_{\text{fum}}-(\text{H})_{\text{aqua}}-\text{O}_{\text{fum}}-\text{C}_4\text{O}-\text{Ni}'$  is also an important pattern exhibited by the crystal structure of **1**. These rings are linked to each other by another type of intra-molecular hydrogen bonded rings of description  $\text{S}(6)$ .

Both  $\text{C}-\text{H}\cdots\pi$  and  $\pi$ - $\pi$  interactions are found to occur in the crystal structure of **1**.  $\text{C}-\text{H}\cdots\pi$  interaction is observed between the pyridyl ring hydrogen of one 4-CNpy and the aromatic  $\pi$  system of another 4-CNpy ligand (Fig. 3). The observed value of  $\text{C}\cdots\pi$  (pyridyl ring centroid) distance for compound **1** is 3.793 Å with a  $\angle\text{C}-\text{H}\cdots\pi$  angle of  $113.80^\circ$ . These values are in good agreement with similar interactions reported earlier by other workers [24,25]. The so called  $\pi$ - $\pi$  interactions are observed between the aromatic  $\pi$ -system of the pyridyl rings and the nitrile  $\pi$ -systems

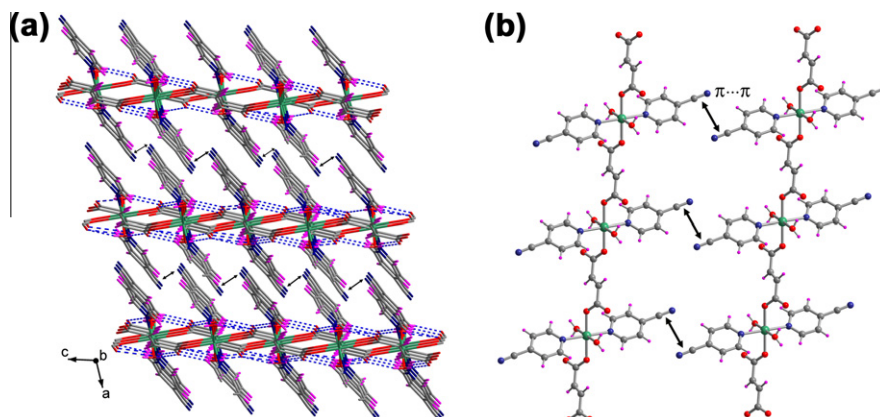


Fig. 4. (a) Line drawing to show overall 3-D supramolecular structure of **1**; (b) Illustration of  $\pi$ (nitrile)– $\pi$ (nitrile) interactions between two adjacent polymeric chains.

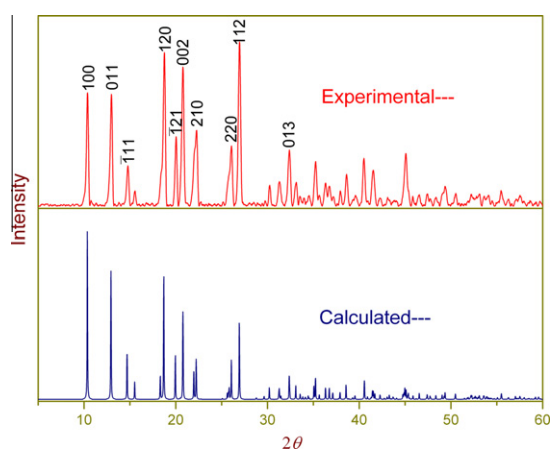


Fig. 5. Observed (top) and simulated (bottom) X-ray powder diffraction patterns of  $[\text{Ni}(\mu\text{-C}_4\text{H}_2\text{O}_4)(4\text{-CNpy})_2(\text{H}_2\text{O})_2]_n$  **1**.

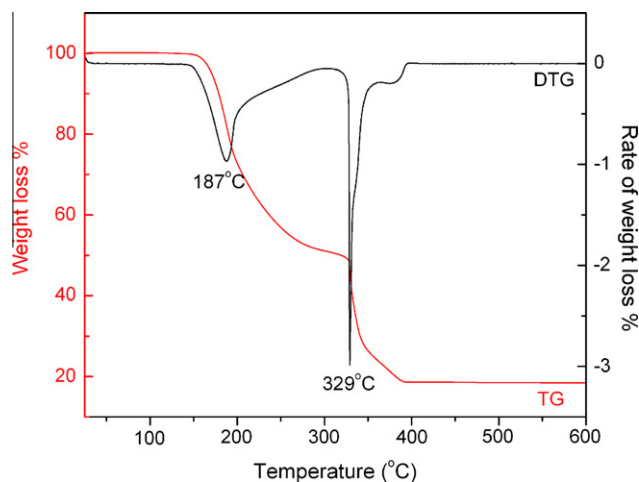


Fig. 7. TG and DTG curves for  $[\text{Ni}(\mu\text{-C}_4\text{H}_2\text{O}_4)(4\text{-CNpy})_2(\text{H}_2\text{O})_2]_n$  **1**.

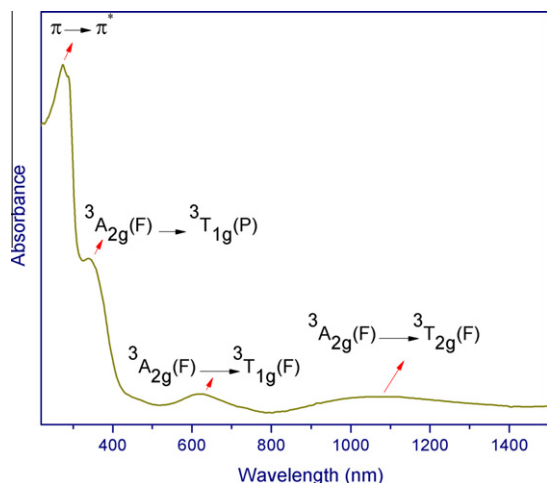


Fig. 6. Solid state UV-vis-NIR spectrum of  $[\text{Ni}(\mu\text{-C}_4\text{H}_2\text{O}_4)(4\text{-CNpy})_2(\text{H}_2\text{O})_2]_n$  **1**.

with centroid···centroid distances of 3.681 Å for compound **1**. In addition, the anti-parallel alignment of nitrile fragments, coming from two different layers also leads to weak  $\pi$ – $\pi$  interactions. The observed  $\text{C}\equiv\text{N}(\text{centroid})\cdots\text{C}\equiv\text{N}(\text{centroid})$  distances for compound **1** is 3.953(3) Å. This kind of  $\pi$ – $\pi$  interactions were also observed in some of our other structures containing 4-CNpy ligands.

Hartree–Fock and DFT calculations were found to support the occurrence of these interactions [12]. As can be seen from Fig. 4a and b, these interlayer  $\pi$ – $\pi$  interactions between anti-parallel nitrile groups extend the supramolecular structure in the 3rd dimension. Indeed, these non-covalent interactions appear to be an important factor for stabilizing the crystal structures of **1**.

### 3.3. Powder X-ray diffraction

All the observed peaks in the experimental powder pattern are seen in the powder pattern calculated on the basis of structural results obtained from single-crystal data. A comparison of experimental and calculated PXRD patterns is shown in Fig. 5. The close similarity between observed and calculated XRD patterns suggests the purity of crystalline bulk sample and also the veracity of the structure described by us. Powder XRD data with  $hkl$  indices for the prominent lines have been determined by comparing the two patterns.

### 3.4. Spectral properties

A powdered sample obtained from light green crystals of  $[\text{Ni}(\mu\text{-C}_4\text{H}_2\text{O}_4)(4\text{-CNpy})_2(\text{H}_2\text{O})_2]_n$  **1** shows three  $d$ – $d$  transitions at 342 nm, 622 nm and 1082 nm (Fig. 6). These are associated with the spin allowed transitions from the  ${}^3A_{2g}$  ground term to the three excited triplet terms viz.,  ${}^3T_{2g}(F)$ ,  ${}^3T_{1g}(F)$  and  ${}^3T_{1g}(P)$  as applicable

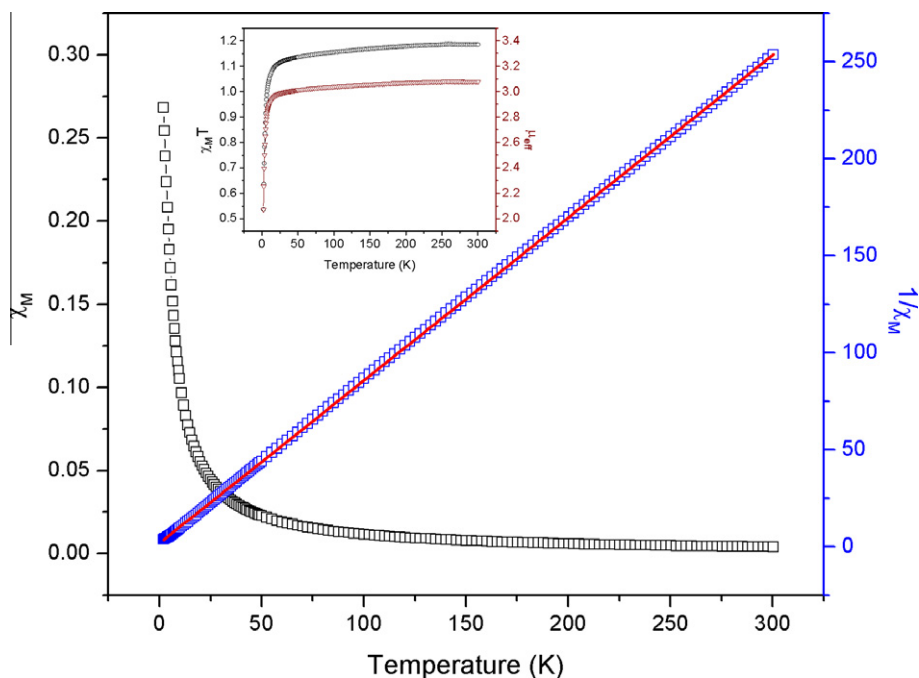


**Fig. 8.** Temperature dependence magnetic susceptibilities and their inverses for  $[\text{Ni}(\mu\text{-C}_4\text{H}_2\text{O}_4)(4\text{-CNpy})_2(\text{H}_2\text{O})_2]_n$  **1**. The inset in the figure shows the variations of  $\chi_M T$  and  $\mu_{\text{eff}}$  with temperature.

for octahedral nickel(II) complexes. The first spin allowed transition, to the  ${}^3T_{2g}(F)$  state occurs at a  $\lambda_{\text{max}}$  value of 1082 nm. The bands at 622 nm and 342 nm are assigned to the transitions to  ${}^3T_{1g}(F)$  and  ${}^3T_{1g}(P)$  states respectively. In addition to this, a band due to  $\pi \rightarrow \pi^*$  transition of pyridine origin appears at 278 nm.

The FT-IR spectrum of compound **1** shows the characteristic  $\nu(\text{C-H})$  stretching vibration of the fumarate ligand at around  $3108\text{ cm}^{-1}$ . The  $[\nu_{\text{as}}(\text{OCO})]$  and  $[\nu_{\text{s}}(\text{OCO})]$  bands appear at  $1542\text{ cm}^{-1}$  and  $1384\text{ cm}^{-1}$  respectively, which are significantly lower than the uncoordinated  $[\nu_{\text{as}}(\text{OCO})]$  and  $[\nu_{\text{s}}(\text{OCO})]$  bands. It also shows two medium intensity bands around  $\sim 805$  and  $\sim 760\text{ cm}^{-1}$  assigned to the OCO bending frequencies. The  $\nu(\text{C=N})$  vibration of the pyridine ring for **1** occurs at  $1608\text{ cm}^{-1}$ . A sharp band appearing at  $2242\text{ cm}^{-1}$  for the compound is assigned to the  $\text{C}\equiv\text{N}$  vibration of the 4-CNpy ligand.

### 3.5. Thermal properties

In the TG curve for compound **1** (Fig. 7), the first step of decomposition involves the release of two 4-CNpy molecules with a weight loss of ca. 49.31% (calculated value is 48.88%) in the temperature range 143–305 °C (bp of 4-CNpy, 196 °C). The most striking aspect of the thermogram is the absence of steps assignable to weight loss due to dehydration. Over the temperature range 310–392 °C, a weight loss of about 32.37% occurs due to the calculated value of 32.13% for the species  $\text{C}_2\text{H}_2$ ,  $\text{CO}_2$ ,  $\text{CO}$  and  $2\text{H}_2\text{O}$ . On heating above 400 °C, the residue left behind is NiO (by PXRD). This proposed pathway however remains tentative. It is possible that before the temperature reaches 305 °C, the water molecules take part in the formation of fumaric acid and also that the resulting hydroxyl groups remain attached to the metal ion as ligands. More detailed studies will be required to establish the above mechanism.

### 3.6. Magnetic properties

The  $\mu_{\text{eff}}$  (300 K) value of 3.08 BM for compound **1** falls within the commonly observed values for six-coordinate high spin Ni(II)

complexes. To determine the temperature dependence of magnetic properties we measured the variable temperature susceptibilities in the temperature range 2–300 K at a constant magnetic field of 1000G. The  $\chi_M$  and  $1/\chi_M$  vs.  $T$  plots are shown in Fig. 8. Theoretical fitting of the  $1/\chi_M$  vs.  $T$  curve using the Curie–Weiss law,  $\chi = C/(T - \Theta)$  (where,  $C$  is the Curie constant and  $\theta$  the Weiss constant), gives a negative  $\theta$  value of  $-2.54\text{ K}$  which suggests antiferromagnetic behavior. The Curie constant,  $C$  for this compound is found to be  $1.19\text{ emu}\cdot\text{K mol}^{-1}$ . Both  $\chi_M T$  vs.  $T$  as well as  $\mu_{\text{eff}}$  vs.  $T$  plots indicate the inherent weakness of the antiferromagnetic exchange interaction. The reported Co(II) complex mentioned above [20] was also found to be weakly antiferromagnetic ( $J = -0.22\text{ cm}^{-1}$ ).

## 4. Conclusion

The ease of isolation of **1** confirms the tendency of the fumarate dianion to act as a bridging spacer in coordination polymers. It is also found that by making use of ancillary ligands like pyridine and substituted pyridines it is possible to generate 1-D coordination polymers. It appears from our study that non-covalent intermolecular interactions like hydrogen bonding,  $\text{C-H}\cdots\pi$  and  $\pi\cdots\pi$  interactions may give extra thermal stability to coordination polymers. Magnetic exchange interaction in the coordination polymer having paramagnetic  $\text{Ni}^{2+}$  ions bridged by the fumarate dianion is weakly antiferromagnetic.

## Acknowledgments

Financial support from University Grants Commission and Department of Science & Technology, India (FIST) is gratefully acknowledged. SJB thanks CSIR, India, for a Junior Research Fellowship awarded to him. The authors also thank Yoshitaka Matsushita of Hyogo, Japan for kindly providing us with the SQUID data and the Department of Chemistry, Indian Institute of Technology, Guwahati for the single crystal X-ray diffraction data. The powder

XRD data were obtained from the DST-SAIF facility, Gauhati University.

### Appendix A. Supplementary material

CCDC 777425 contains the supplementary crystallographic data for **1**. These data can be obtained free of charge via <http://www.ccdc.cam.ac.uk/conts/retrieving.html>, or from the Cambridge Crystallographic Data Centre, 12 Union Road, Cambridge CB2 1EZ, UK; fax: +44 1223 336 033; or e-mail: [deposit@ccdc.cam.ac.uk](mailto:deposit@ccdc.cam.ac.uk). Supplementary data associated with this article can be found, in the online version, at [doi:10.1016/j.molstruc.2011.05.039](https://doi.org/10.1016/j.molstruc.2011.05.039).

### References

- [1] F.R. Keene, Dalton Trans. 40 (2011) 2405–2418.
- [2] R.K. Barman, B.K. Das, CrystEngComm 14 (2002) 1–4.
- [3] G.R. Desiraju, Acc. Chem. Res. 29 (1996) 441–449.
- [4] G.R. Desiraju, Curr. Sci. 81 (2001) 1038–1042.
- [5] N. Guillou, S. Pastre, C. Livage, G. Férey, Chem. Commun. (2002) 2358–2359.
- [6] S. Konar, E. Zangrando, M.G.B. Drew, J. Ribas, N. Ray Chaudhuri, Dalton Trans. (2004) 260–266.
- [7] A.Y. Robin, K.M. Fromm, Coord. Chem. Rev. 250 (2006) 2127–2157.
- [8] L. Pan, M.B. Sander, X. Huang, J. Li, M. Smith, E. Bittner, B. Bockrath, J.K. Johnson, J. Am. Chem. Soc. 126 (2004) 1308–1309.
- [9] Y.K. Lee, S.W. Lee, Bull. Korean Chem. Soc. 24 (2003) 906–910.
- [10] F. Bigdeli, A. Morsali, Mater. Lett. 64 (2010) 4–5.
- [11] B. Folch, J. Larionova, Y. Guari, L. Datas, C. Guérin, J. Mater. Chem. 16 (2006) 4435–4442.
- [12] B.K. Das, S.J. Bora, M.K. Bhattacharyya, R.K. Barman, Acta Cryst. B56 (2009) 467–473.
- [13] *Origin*® 8: The Data Analysis and Graphing Workspace, Originlab Corporation, One Roundhouse Plaza, Northampton, MA, USA, 2007.
- [14] *SMART/SAINT*: Bruker AXS Inc., Madison, Wisconsin, USA, 2004.
- [15] G.M. Sheldrick, Acta Cryst. A64 (2008) 112–122.
- [16] L. Farrugia, J. Appl. Cryst. 32 (1999) 837–838.
- [17] L. Farrugia, J. Appl. Cryst. 30 (1997) 565.
- [18] K. Brandenburg, Diamond 3.1f, Crystal Impact GbR, Bonn, Germany, 2008.
- [19] W. Kraus, G. Nolze, PowderCell for Windows, Ver. 2.4, Federal Institute for Materials Research and Testing, Berlin, 2000.
- [20] K.-L. Zhang, Trans. Met. Chem. 30 (2005) 376–379.
- [21] Y.-Q. Zheng, J.-L. Lin, B.-Y. Chen, J. Mol. Struct. 646 (2003) 151–159.
- [22] J.-F. Ma, J. Yang, J.-F. Liu, Acta Cryst. E59 (2003) m900–m902.
- [23] J. Bernstein, R.E. Davis, L. Shimon, N.-L. Chang, Angew. Chem. Int. Ed. Engl. 34 (1995) 1555–1573.
- [24] T.J. Prior, M.J. Rosseinsky, CrystEngComm 24 (2000) 128–133.
- [25] C.S. Lai, F. Mohr, E.R.T. Tiekink, CrystEngComm 8 (2006) 909–915.